

All-silicon waveguides and bulk etched alignment structures on (110) silicon for integrated micro-opto-mechanical systems

Steven W. Smith, Mehran Mehregany, Frank Merat and David A. Smith

Case Western Reserve University, Department of Electrical Engineering & Applied Physics
Cleveland, Ohio 44106-7221

ABSTRACT

We present the first large-area, all-silicon rib waveguides and fiber guiding U-grooves fabricated on (110) silicon substrates. Waveguide rib structures with a height of $6.7\mu\text{m}$ and widths of 5, 10, and $15\mu\text{m}$ are RIE etched into a lightly-doped epitaxial silicon layers deposited on a heavily doped silicon substrates. Fiber-guiding U-grooves with unique corner compensation structures are anisotropically etched by a 35 wt.% KOH solution at 70°C , with and without ultrasonic agitation of the etching solution. Devices fabricated without ultrasonic agitation have a U-groove bottom surface roughness (Ra) of 5606\AA , while devices with ultrasonic agitation have a surface roughness (Ra) of 341\AA . Ultrasonic etching improves the surface roughness of the U-groove bottoms by a factor of 16.4. We found that the variation of U-groove etch depth is greater than $1\mu\text{m}$ across the wafer, even with ultrasonic agitation of the etchant. Examination of the waveguide modal structure indicates that devices with $6.7\mu\text{m}$ tall and $10\mu\text{m}$ wide rib structures propagate only one waveguide mode at 1550nm . The total loss of the straight waveguides was as low as 4.88 dB, and the propagation loss was estimated to be 1.68 dB. These loss values indicate waveguide end-faces fabricated by anisotropic etching of (110) silicon do not need to be polished.

Keywords: all-silicon waveguides, U-grooves, fiber optics, micro-opto-mechanical systems, MEMS, KOH etching, (110) silicon

2. INTRODUCTION

We are developing integrated micro-opto-mechanical systems (MOMS) combining integrated optics (IO) with bulk-micromachined alignment structures, and optical elements on micro-electrical-mechanical components.¹ The fabrication of typical silica IO devices requires specialized flame-hydrolysis-deposition (FHD) systems which deposit thick ($20\mu\text{m}$) oxide layers. The FHD process is incompatible with many integrated circuit (IC) and micromachining processes. A silicon waveguide technology would be more compatible with both IC and micromachining technology and would open up a broad range of new applications for micromachining, micro-optics and integrated optics. Unfortunately, unacceptable levels of optical loss in silicon waveguides ($>10\text{ dB/cm}$) have been an obstacle to the successful implementation of single-mode, all-silicon waveguides. This problem has been surmounted with the recent development of large-area, all-silicon waveguides having a propagation loss of approximately 1 dB/cm .²⁻⁴ This all-silicon waveguide technology is an enabling technology compatible with bulk and surface micromachining processes used in the fabrication of micro-mechanical devices on silicon. In addition to favorable processing characteristics, the technology is suitable for production of optical modulators which exploit silicon's thermal properties and charge carrier effects.⁵⁻⁸ These new active optical elements permit a wide range of applications for all-silicon IO technology. We envision using this waveguide technology for optically interconnecting micro-electrical-mechanical devices fabricated on a silicon wafer. In this paper we report the first all-silicon waveguides fabricated on (110) silicon substrates.

When silicon substrates with (110) orientation are bulk etched in a KOH solution, the substrate's (111) crystal planes are exposed, allowing the formation of optically smooth waveguide end-faces. These crystal planes can also be exploited to form passive mirrors, beam splitters and laser diode tuning cavities.⁹ Such smooth end-faces eliminate the need for mechanical polishing of waveguide, a problem which significantly increases the cost of all-silicon IO devices on (110) silicon. In this paper we demonstrate that loss values obtained from all-silicon waveguides with anisotropically etched end-faces are only 0.18 dB larger than the loss values from all-silicon waveguides fabricated on (100) silicon substrates.³

Several clever schemes exist for coupling light from fiber cables into integrated optical systems, including surface-micromachined alignment mirrors and bulk-etched guiding grooves.¹⁰ Guiding grooves are useful for coupling light into optical waveguides, and as a method to simplify the alignment and assembly of micro-optical components.¹¹ At a minimum, three methods for realizing the grooves have been explored, including bulk-etched silicon V-grooves, isotropically etched silicon U-grooves, and RIE etched silica grooves.¹²⁻¹⁴ In this paper we examine the feasibility of using anisotropically etched (110) silicon U-grooves as alignment structures for fiber optical cables. The unique crystal structure of (110) silicon substrates allows high aspect-ratio, U-shaped trenches to be etched into the silicon substrate.¹⁵ We have developed a unique corner compensation structure which allows long, straight U-grooves to be anisotropically etched in the (110) silicon substrates. These U-grooves allow fiber cables to be aligned to waveguides. Additionally, the angle at which the waveguide end-faces are etched eliminates unwanted Fabry-Perot cavities from being formed between the fiber cable and waveguide end-faces.¹⁶ The all-silicon waveguides developed in this paper do not yet use U-grooves and are positioned between two, parallel (111) crystal planes, which are vertical to the (110) substrate. This allows the devices to be tested separately from the fiber guiding U-grooves. We plan to combine the U-groove devices with the all-silicon waveguides for passive alignment of fiber cables to waveguides. The U-grooves will provide a means of aligning laser diodes and detectors to the waveguides devices.

3. DESIGN

3.1 Waveguide Design

Large-area all-silicon waveguide technology requires the formation of rib waveguides with large cross-sections. The rib waveguide's lower cladding layer is created by doping the silicon substrate with an high concentration of phosphorous, lowering the substrate's optical index. Then the core layer is formed by depositing a 20 μm epitaxial layer of low-doping concentration on the silicon substrates.¹⁷ A rib is etched into the epitaxial layer, geometrically confining the light in the horizontal direction. This rib is etched to a depth selected to obtain single mode behavior, following criteria suggested by previous researchers.²⁻⁴ The devices fabricated for this paper have rib widths which range from 5 to 15 μm and are etched to a depth of 6.7 μm .

To support only the fundamental waveguide mode, the cross-sectional dimensions of the waveguide rib must not be similar to the dimensions of a single-mode slab waveguide.³ Only one HE_{00} mode can theoretically propagate when the ratio of the rib width to the rib height is chosen correctly and any higher order modes couple into the slab section of the waveguide. The criterion for single-mode operation can be stated as

$$\frac{w}{h} \leq 0.3 + \frac{r}{\sqrt{1-r^2}} \quad (1)$$

where w is the width of the rib, h is the height of the rib, and r is the ratio of lateral slab height to rib height. For the waveguides developed in this paper, the height is 20 μm , and the rib width ranges from 5 to 15 μm . The ratio of rib width to height for the 15 μm wide rib is 0.75 and satisfies equation 1. Therefore all of the waveguides discussed in this paper theoretically support only a single waveguide mode.

3.2 U-groove Design

The shape of a cavity which is etched into a (110) silicon substrate is dependent on the shape and orientation of the pattern opened in the masking film. There are four (111) crystal planes which intersect the (110) substrate surface at 90° but not at right angles to each other. Two additional crystal planes intersect the substrate surface at an angle of 35.26° . When a cavity is anisotropically etched through a rectangular opening in the etch mask, a six-sided structure is etched into the substrate which is bounded by these (111) planes.¹⁸ To fabricate vertical U-grooves in silicon, the photolithography mask openings must be aligned parallel to two of the planes that intersect the wafer surface at 90° . If the mask opening is misaligned from the (111) planes, it will undercut to a new width

$$w' = L \sin(\theta) + w \cos(\theta) \quad (2)$$

where L is the length of the mask opening, θ is the angular misorientation, and w is the original width of the etch-window. The maximum depth to which the cavity will etch is

$$depth = \frac{a + b\sqrt{2}}{2\sqrt{6}} \quad (3)$$

where a is the width of the etched slot, and b is the length of the etched slot.¹⁹ To align the photolithography masks to the silicon substrate, a fan pattern is etched into the silicon and the following masking layers are aligned to the fan groove with the minimum undercutting which defining the direction of the (111) planes.²⁰

To align a fiber optical cable to an optical waveguide using a U-groove, corner compensation structures must be added to the U-groove design. This prevents the (111) plane which slants at 35.26° from the (110) surface from forcing the fiber cable out of the U-groove as it approaches the waveguide's end-face. A U-groove mask design with corner compensation openings is shown in Figure 1. The width of the U-grooves must be at least $128\mu\text{m}$ (125 ± 3) to accommodate a standard single mode fiber-optical cable. The etch depth should be selected to place the fiber optical cable under the rib of the waveguide. This suggests that the depth should be greater than $66.5\mu\text{m}$ and less than $82.5\mu\text{m}$. This optimum depth is best obtained experimentally and must be carefully controlled to place the level of the fiber core within $\pm 0.5\mu\text{m}$ of the optimum position for coupling light into the waveguides.

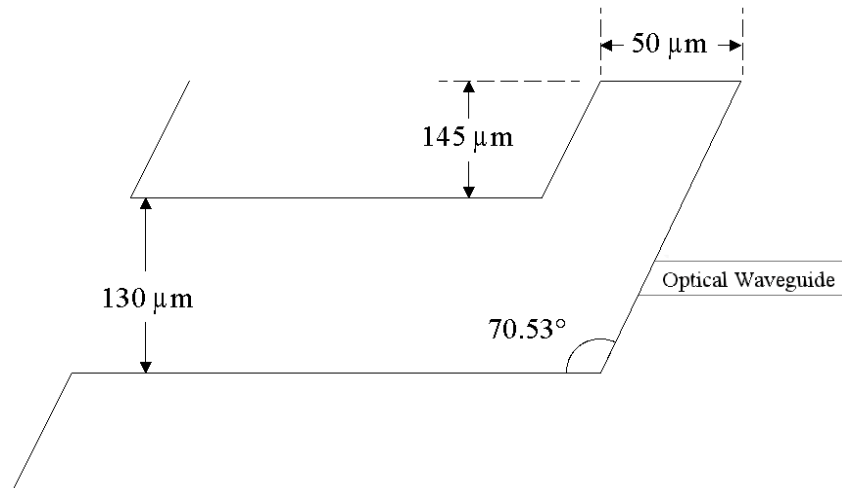


Figure 1. Schematic (plan view) of a mask opening used to etch fiber guiding U-grooves, complete with dimensions used to fabricate the devices. Note the dimension of the fiber opening is larger than the minimum value to allow for unimpeded placement of fibers into the grooves.

4. PROCESSING

4.1 Fabrication Process

Fabrication begins with 4" (110) silicon wafers having an n-type-phosphorous doping level of 10^{19} cm^{-3} . These wafers have a resistivity of 0.001 to 0.003 ohm-cm and an optical index of refraction of 3.49 at 1500 nm. Then a 20 μm thick layer of epitaxial silicon with a doping level of less than 10^{15} cm^{-3} is deposited on the silicon wafers. This silicon layer has a conductivity of 4.5 ohm-cm and a refractive index of 3.5 at 1500 nm. The n-type substrate doping is chosen to allow for anisotropic etching, as heavy p-type doping will act as an etch stop for usual bulk silicon etchants.²¹ The doping concentrations are chosen to match the work of previous researchers to allow for a comparison with their results.³

After epitaxial deposition, a 0.5 μm masking film of thermal SiO_2 is grown on the substrate. Next, a fan-shaped series of openings are photolithographically patterned. The exposed silicon is anisotropically etched in 17 wt. % KOH at 55° to produce long, narrow U-grooves in the silicon substrate (Fig 1 (a)). The fan patterns consist of openings, which are 8 μm wide and 3000 μm long, spaced at angular intervals of 0.1° from negative 2.5° to positive 2.5°. By examining the degree of oxide undercut for each of these openings, the direction of the (111) crystal planes can be determined to within 0.1°. The opening with the least amount of undercutting is used for alignment of subsequent mask layers to the (111) planes. Subsequent to the fan pattern etching, the waveguide ribs are patterned and etched into the epitaxial silicon layer using Cl_2 reactive-ion-etching (Fig. 1 (b)). Etching depth is selected to be 6.7 μm by timed endpoint. The Cl_2 recipe benefits from high selectivity between the SiO_2 etch mask and the (110) silicon etch rate, producing nearly square rib profiles.

The 6.7 μm rib heights present a problem for subsequent processing steps as their large step height causes poor photoresist step coverage. This step coverage problem allows HF to attack the oxide mask layer which protects the waveguide ribs during U-groove pattern delineation. Subsequent KOH etching of the U-groove structures would, in turn, destroy the waveguide rib structures. This problem is corrected by use a thick photoresist process. This process, developed by other researchers in our laboratories, using AZ4620 photoresist provides adequate step coverage for subsequent etching steps.²² Then, the U-grooves are etched using a 38 wt. % KOH solution at 70° C. (Fig. 1 (c)). This etch recipe provided the smoothest sidewalls and groove bottoms.²³

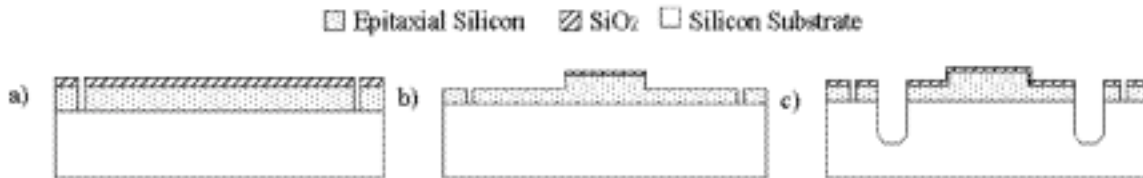


Figure 1. Schematic of the fabrication process for the all-silicon waveguides and U-grooves.

4.2 Processing Results

The fan patterns were used to successfully determine the direction of the (111) crystal planes and the waveguide ribs were then aligned to the (111) direction to within 0.1°. The waveguide ribs were formed by RIE etching using Cl_2 chemistry, which produced nearly square rib profiles with a sidewall slope angle of approximately 83°. The sides of the rib structure were found to be visibly smooth when examined with a scanning electron microscope (SEM). This indicates the waveguides should not have excessive loss because a major obstacle to formation of low-loss waveguides is excess scattering due to rib surface roughness. Figure 2 shows a step profile silicon, as measured with the Sloan Dektac 3030ST, of a rib etched in the epitaxial. Both discontinuities in the step profile are due to the pointed tip of the Dektac's stylus and not to any discontinuity in the etch profile.

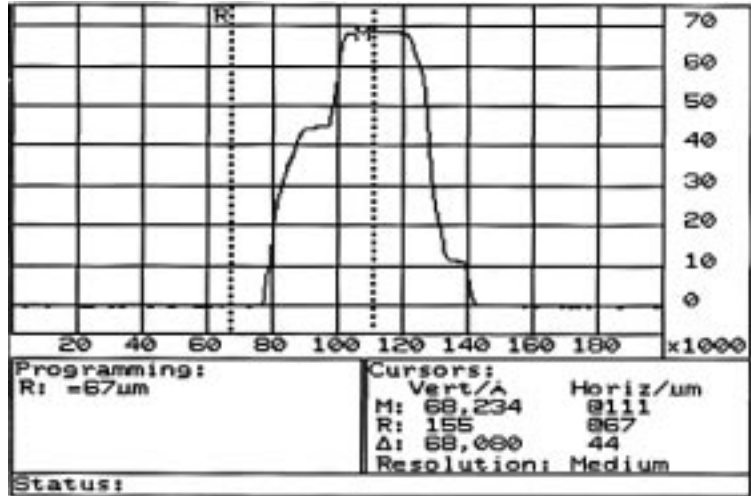


Figure 2. Dektac step profile measurement of a typical waveguide rib. The height of the rib structure is 6.7μm.

Initial U-groove fabrication results show that the formation of fiber guiding U-grooves in (110) silicon substrates is achievable. The corner compensation structures prevent the slanted crystal planes from entering the fiber guiding channel, as expected. Figure 3(a) shows an SEM photograph of two anisotropically etched U-grooves which can align optical fibers to waveguide ribs. Figure 3(b) shows a close-up of a U-groove opening. Figure 4 shows the vertical rib profile obtained with Cl₂, and the high quality end-face obtained with ultrasonic KOH etching.

Controlling the depth variation to better than 1μm is not currently possible by the fabrication techniques available at CWRU. The depth of the U-grooves is easily controlled to within 3μm by careful timing of the etch depth, but the variation of etch depth across a wafer is at best 3μm. Through process development, the variation in effective U-groove depth should be controllable to within 1μm. We are investigating in-situ monitoring of etch stop techniques to accurately control the U-groove depth.

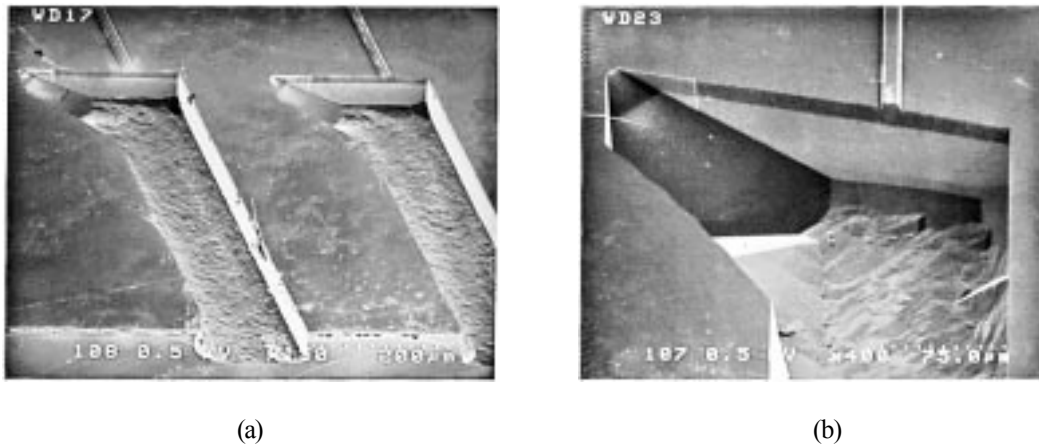


Figure 3. Anisotropically etched U-grooves, without ultrasonic agitation, for input to rib waveguides, (a) and close up of one of the U-groove structures, (b). Note the corner compensation structure and the (111) plane slanted at 35° to the substrate surface.

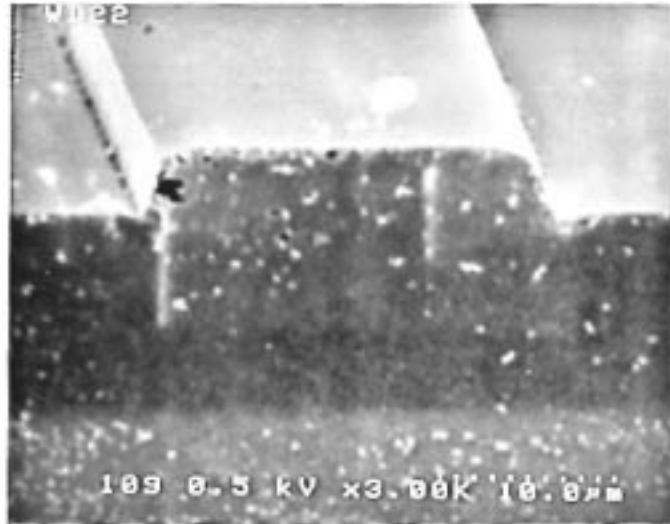
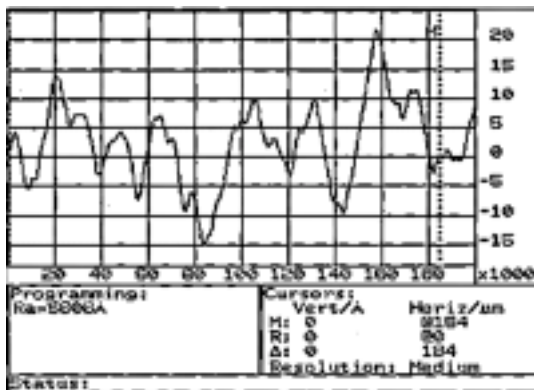
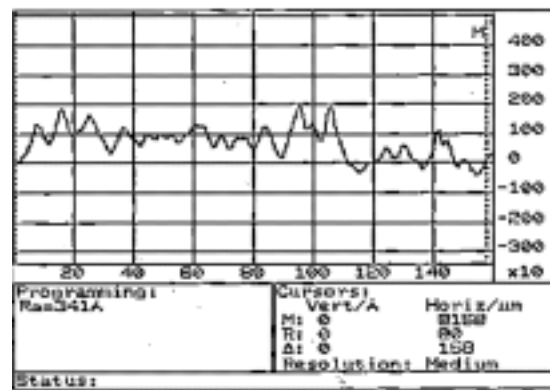


Figure 4. Anisotropically etched end-face of an all silicon waveguide. Note the darker gray of the epitaxial silicon and the lighter gray of the highly doped substrate caused by the conductivity difference between the silicon layers.

The surface roughness of the fabricated U-groove bottoms is not satisfactory for applications demanding strict control of the etch depth, such as passively coupling light from fiber optical cables into waveguides. The surface roughness on the groove bottom is due to bubble formation during the etch process. Ultrasonically agitation of the etching solution has been employed by other researchers to eliminate bubble formation producing uniform, smooth etch profiles.²⁵ The average surface roughness of a typical U-groove bottom is 5606 Å as measured with the Dektac, with roughness values as high as 6.2µm for some samples. Additionally, new results have shown that anisotropic etching with KOH may not provide optically smooth (111) crystal planes.²⁶ Measurement of the surface roughness of the crystalline faces is difficult but SEM photographs reveal that the surface is smooth enough for many optical applications, such as optical mirrors and coupling of fibers to waveguide end-faces. To compare results from usual KOH etching techniques with ultrasonic wet etching, a device wafer was etched in a 34 wt % bath of ultrasonically agitated KOH at 70°C (Branson Ultrasonic Cleaning system Model S8040-12 and Model C1012-40-12). After ultrasonic etching was applied, the U-groove bottoms had a typical surface roughness (Ra) of 341 Å. Figure 5 shows surface profile data taken with the Dektac for a etched U-groove bottom without ultrasonic agitation and a etched U-groove bottom with ultrasonic agitation of the etching solution. The advantages of the ultrasonic agitation are clear, as the surface roughness is reduced by a factor of 16.4.



(a)



(b)

Figure 5. Measurements of U-groove bottom roughness from (a) normally KOH etched U-groove, and (b) ultrasonically KOH etched U-groove. Note the value of the surface roughness (Ra) for each of the etching techniques.

Improvement is also evident in the processing of the waveguide devices when ultrasonic etching is used during U-groove fabrication. The substrates have visibly fewer surface particulates and much less undesired etching damage. The overall quality improvement is clear when Figure 3(a) is compared to Figure 6(a), which shows a U-groove pair fabricated with ultrasonic etching. The decrease in the surface-roughness of the U-groove bottom is evident upon comparison of the U-groove bottoms in Figure 3(b) and Figure 6(b), which is a close up SEM picture of the opening end of a U-groove. Finally, the high quality of the waveguides is very clear upon examination of the rib waveguide shown in Figure 7. Fiber optical cables fit into the U-grooves without difficulty, but the U-grooves can not accurately align the cable in the vertical or horizontal directions due to the processing variations.

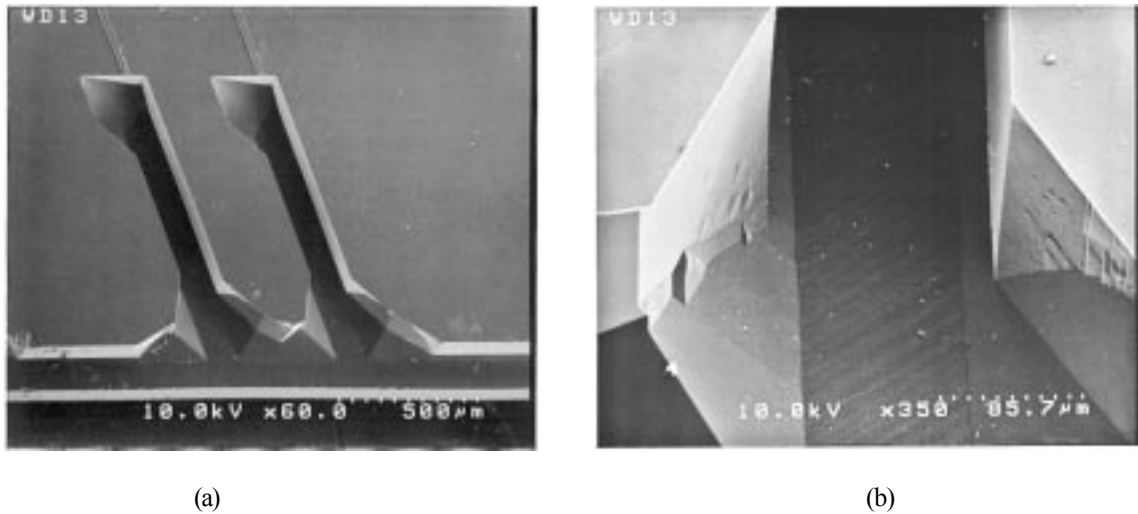


Figure 6. Ultrasonically etched U-grooves for input to (a) waveguide ribs, and (b) close-up of the start of one of the U-grooves. The etch depth is $134\mu\text{m}$, and the unusual shape of the opening is due to undercutting at the intersection of the die-dicing channel and the U-groove.

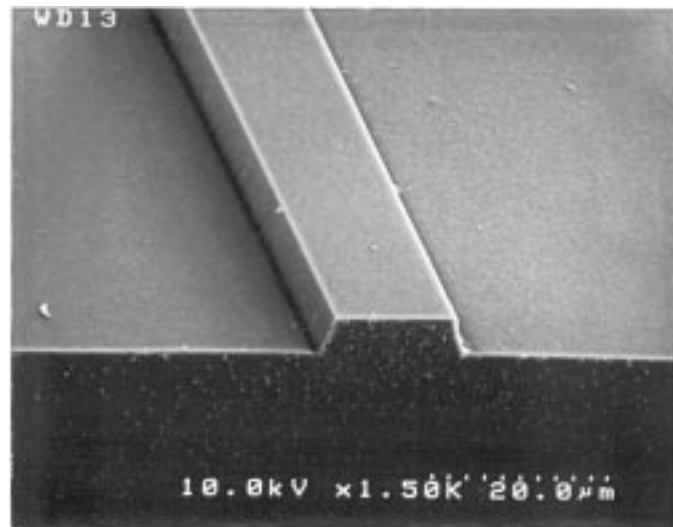


Figure 7. Ultrasonically etched end-face of a rib waveguide with a rib height of $6.7\mu\text{m}$, a base width of $15.5\mu\text{m}$ and an etch angle of 83.6° .

5. OPTICAL TESTING

5.1 Optical mode testing

By examining the intensity profile of the output light beam, the difference between single and multi-mode waveguides can be determined. Once the data for the optical beam profile is collected, the data is converted into a three-dimensional beam profile. To determine whether the large area waveguide structures are single-mode or multi-mode, an IR CCD camera is used. If the beam appears to have a gaussian intensity profile and is insensitive to small variations in input coupling, then there is strong evidence that the waveguide is a single-mode device. Figure 8 shows a schematic of the test setup used to measure the modal field distribution in the all-silicon waveguides.

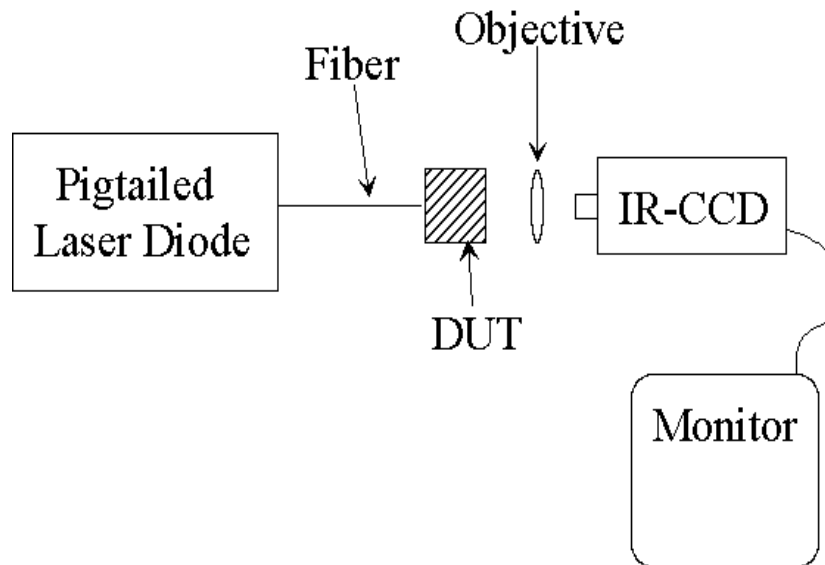


Figure 8. Schematic of the setup used to examine the laser beam profiles of the all-silicon waveguides. Photographs of the monitor output were taken to record the laser beam spots.

Initial experiments were performed on straight waveguides with a $6.7\mu\text{m}$ high and $10\mu\text{m}$ wide rib using a distributed feedback laser operating at a wavelength of 1531 nm . During these experiments, multiple optical modes of the waveguide were never seen as the position of the input fiber was varied. This is important because dramatic changes in the modal structure of multi-mode waveguides are typically visible when the input coupling conditions change. Figure 9(a) shows a far-field photograph of the output beam from such a waveguide and Figure 9(b) shows the three-dimensional profile of this beam's optical intensity. This profile provides strong evidence that our large area waveguides are single-mode devices because they have a gaussian-like intensity distribution. The beam is narrower in the vertical direction than in the horizontal direction due to the dimensions of the waveguide ribs and the epi-layer thickness. These results are promising, because the all-silicon waveguide technology is appropriate for single-mode optical systems.

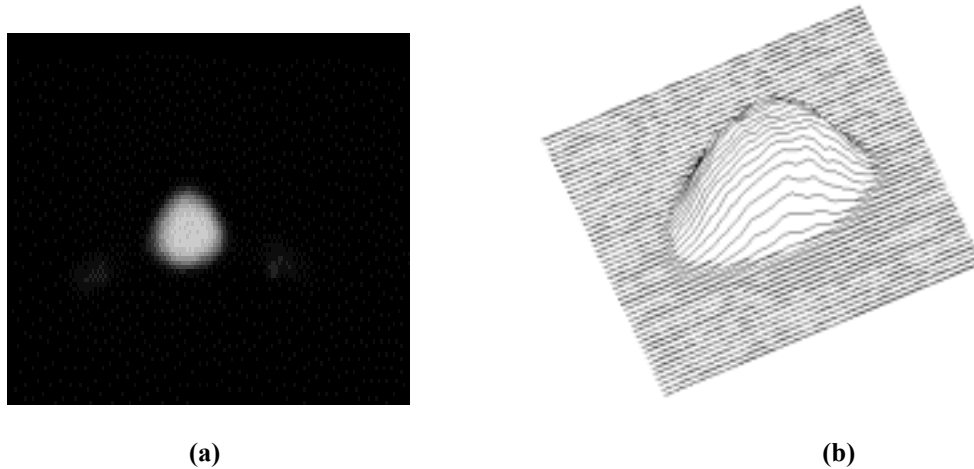


Figure 9. Photograph of (a) the laser beam profile from a rib waveguide with a $6.7\mu\text{m}$ tall rib and (b) its three-dimensional intensity profile.

5.2 Optical Loss testing

An optical fiber was placed next to the end of the waveguide, and 1531nm light from a distributed feedback laser coupled into the epi-layer. A CCD camera and microscope objective were used to align the fiber to the waveguide end-face. Once aligned, a large area photodetector, neutral density filter, and a variable aperture are used to measure the optical intensity of the beams. The signal from the photodetector was amplified and measured using a digital multi-meter to obtain the optical intensity. Figure 10 shows a schematic of the optical loss testing set-up used to measure the loss characteristics of the waveguides. These measurements provide valuable information as to how the devices will perform as components in an optical system, but cannot be used to separate the total loss into the individual contributions from end-face scattering, reflection, and propagation-loss.

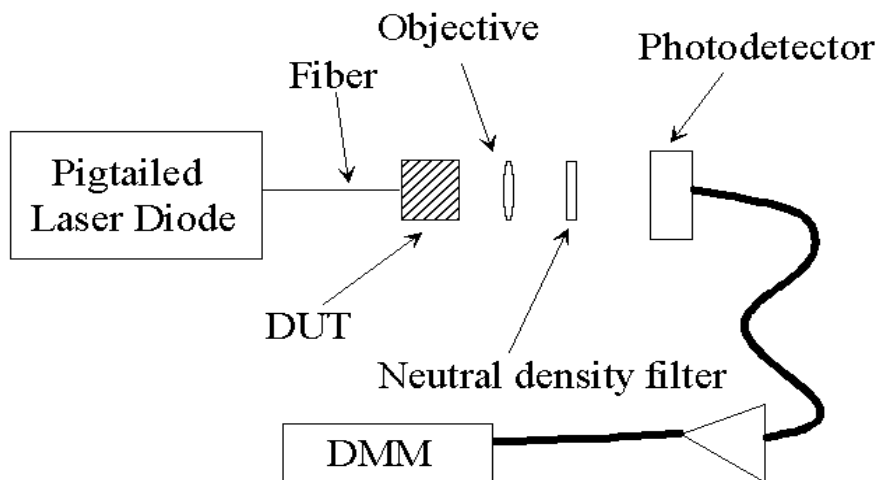


Figure 10. Schematic of experimental setup used to measure optical propagation loss.

Results from loss measurements are comparable to the results obtained by Splett and Petermann.³ Their best total loss measurement was given as 4.7 dB total loss for waveguides with $15\mu\text{m}$ wide ribs. Their waveguides required end-face polishing because they were formed on (100) silicon wafers, while our waveguides with anisotropically etched end-faces do not require mechanical polishing to obtain results very similar to their polished waveguides. Since little difference in intensity results due to polarization variation

was noted in the published literature, the polarization dependence of the devices was not investigated. Table 1 shows the results of loss waveguide testing from the all-silicon waveguides.

Waveguide Width (μm)	Total Loss (dB)	Propagation Loss (dB/cm)
5	8.32	5.22
10	6.59	3.39
15	4.88	1.68

Table 1. Results of optical loss measurements from all-silicon optical waveguides. Propagation loss is estimated in a similar manner to the methods of Soref and Petermann, that is, subtracting 1.6 dB for Fresnel-loss and 1.6 dB of mode mismatch at the other end.

6. DISCUSSION & CONCLUSIONS

Fabrication of rib waveguide structures with $6.7 \pm 0.2\mu\text{m}$ tall ribs was achieved. A thick photoresist process prevented damage to the tall rib structures during KOH etching of the fiber guiding U-groove structures. Surface roughness (Ra) for a typical fiber guiding U-groove was measured at 5606\AA . Ultrasonic agitation of the KOH etch bath reduced this number by 16.4 times to a value of 341\AA . U-grooves were KOH etched to a 134\AA depth without damage to the waveguide rib structures, but control of the etch depth was very difficult to achieve. Cleaved fiber-optic cables were found to fit in the bulk etched U-groove structures, but U-groove devices were not able to passively align a fiber to a waveguide end-face horizontally or vertically without complex process development.

All-silicon waveguide devices which were perpendicular to the (111) planes performed well optically and had loss values which were comparable to results obtained for similar waveguides fabricated in (100) silicon. The total loss for these 1 cm long waveguides was measured at 4.88 dB, which is an acceptable amount of loss for many applications. These applications include mass produced systems where very low (<1 dB/cm) optical loss is less important than device cost (disposable biochemical sensors, for example). Waveguides with $6.7\mu\text{m}$ tall waveguide ribs have intensity profiles which appear to be single-mode and are insensitive to small variations in input coupling.

All-silicon waveguides are useful for many optical applications which require low-cost, batch-fabricated IO devices. The choice of (110) substrates may eliminate many of the problems caused by end-face roughness, but KOH etched U-grooves do not yet meet today's standards of passive fiber guiding grooves. All-silicon devices will have applications for low-cost sensors, optical modulators, and micro-optical-mechanical systems (MOMS). Many packaging and fabrication problems still must be overcome before MOMS products containing all-silicon waveguides become high-volume, low-cost products. Also, a more thorough optical modeling and characterization effort must be completed before the optical properties of the devices can be completely optimized.

7. ACKNOWLEDGMENTS

The authors would like to thank Dr. Z. Bao, M. Patan, and H. Rashid of Case Western Reserve University, for assistance in optical testing. We would also like to thank Dr. Jim Harris, and Fred Discenzo of Reliance Electric for providing the impetus for this research. This work was supported in part by ARPA under Contract No. F49620-94-C-0007 and by NSF under Grant No. ECS-9109343.

8. REFERENCES

1. Frank Merat and Mehran Mehregany, "Integrated micro-opto-mechanical systems," In Proceedings SPIE, Vol. 2383, Miniaturized Systems with Micro-Optics and Micromechanics, Feb. 1995.

2. R.A. Soref, J. P. Lorenzo, "Single-Crystal Silicon: A New Material for 1.3 and 1.6 μm Integrated-Optical Components," *Electronics Letters*, Vol. 21, No. 21, pp. 953-954, Oct. 10, 1985.
3. Soref, J. Schmidtchen, and K. Petermann, "Large Single-Mode Rib Waveguides in GeSi-Si and Si-on-SiO₂," *IEEE Photonics Technology Letters*, Vol. 6, No. 3, pp. 1971-1974, Mar. 1994.
4. A. Splett and K. Petermann, "Low Loss Single-Mode Optical Waveguides with Large Cross-Section in Standard Epitaxial Silicon," *IEEE Photonics Technology Letters*, Vol. 6, No. 3, pp. 425-427, Mar. 1994.
5. J.P. Lorenzo, R. A. Soref, "1.3 μm electro-optic silicon switch," *Appl. Phys. Lett.* Vol. 51, No. 1, pp. 6-8, Jul. 6, 1987.
6. B.R. Hemenway, O. Solgaard, and D.M. Bloom, "All-silicon integrated optical modulator for 1.3 μm fiber-optic interconnects," *Appl. Phys. Lett.*, Vol. 55, No. 4, pp. 349-350, Jul. 24, 1989.
7. G. V. Treyz, "Silicon Mach-Zehnder Waveguide interferometers operating at 1.3 μm ," *Electronics Letters*, Vol. 27, No. 2, pp. 118-120, Jan. 17, 1991.
8. G. Cocorullo, M. Iodice, I. Rendina, and P. M. Sarro, "Silicon Thermo-optical Micromodulator with 700-kHz -3-dB Bandwidth," *IEEE Photonics Technology Letters*, Vol. 7, No. 4, pp. 363-365, Apr., 1995.
9. Yuji Uenishi, Masahiro Tsugai, and Mehran Mehregany, "Micro-Opto-Mechanical Devices Fabricated by Anisotropic Etching of (110) Silicon," *IEEE MEMS-94 Workshop*, (Oiso Prince Hotel, Kanagawa, Japan, Jan. 1994.
10. O. Solgaard, M. Daneman, N. C. Tien, A. Friedberger, R. S. Muller, and K. Y. Lau, "Optoelectronic Packaging Using Silicon Surface-Micromachined Alignment Mirrors," *IEEE Photonics Technology Letters*, Vol. 7, No. 1, pp. 41-43, Jan. 1995.
11. M. F. Dautartas, A. M. Benzoni, Y. C. Chen, G. E. Blonder, B. H. Johnson, C. R. Paola, E. Rice, and Y.-H. Wong, "A Silicon-Based Moving Mirror Optical Switch," *IEEE Journal of Lightwave Technology*, Vol 10, No. 8, pp. 1078-1085, Aug. 2, 1992.
12. H. P. Hsu, A. F. Milton, "Flip-Chip approach to Endfire Coupling Between Single-mode Optical Fibers and Channel Waveguides," *Electronics Letters*, Vol. 12, No. 16, pp. 404-405, Aug. 1976.
13. Grand, H. Denis and S. Valette, "New Method for Low Cost and Efficient Optical Connections Between Singlemode Fibers and Silica Guides," *Electronics Letters*, Vol. 27, No. 1, pp. 17-18, Jan. 1991.
14. Yamada, M. Kawachi, M. Yasu, M. Kobayashi, "Optical-fiber coupling to high-silica channel waveguides with fiber-guiding grooves," *Electronics Letters*, Vol. 20, No. 8, pp. 313-314, Apr. 1994.
15. D. L. Kendall, "On etching very narrow grooves in silicon," *Appl. Phys. Lett.*, Vol. 26, No. 4, pp. 195-198, Feb. 15, 1975.
16. I. Ogawa, Y. Yamada, H. Terui, "Reduction of Waveguide Facet Reflection in Optical Hybrid Integrated Circuit Using Saw-Toothed Angled Facet," *IEEE Photonics Technology Letters*, Vol. 7, No. 1, pp. 44-46, Jan 1995.
17. Ernest Bassous, "Fabrication of Novel Three-Dimensional Microstructures by the Anisotropic Etching of (100) and (110) Silicon," *IEEE Transactions on Electron Devices*, Vol. ED-25, No. 10, 1178-1185, Oct. 1978.
18. Elie S. Ammar and T.J. Rodgers, "UMOS Transistors on (110) Silicon," *IEEE Transactions on Electron Devices*, Vol. ED-27, No. 5, pp. 907-914, May 1980.
19. D. R. Ciarlo, "A latching accelerometer fabricated by the anisotropic etching of (110) oriented silicon wafers," *Journal Micromechanical Microengineering*, Vol. 2, pp. 10-13, Feb. 1992.
20. Keiichi Smimaoka, Osamu Tabata and Susumu Sugiyama, "Etch Stop Technique of Polysilicon," *10th Sensor Symposium*, pp. 25-28, 1991.

21. Yuji Uenishi, Masahiro Tsugai, and Mehran Mehregany, "Micro-Opto-Mechanical Devices Fabricated by Anisotropic Etching of (110) Silicon," IEEE MEMS-94 Workshop, (Oiso Prince Hotel, Kanagawa, Japan, Jan. 1994
22. H. Miyajima and M. Mehregany, "High Aspect-Ratio Photolithography for MEMS Applications," submitted to J. Micromechanical Systems.
23. T. A. Kwa, P.J. French, and R. F. Wolffenbuttel, "Anisotropically Etched Silicon Mirrors for Optical Sensor Applications," J. Electrochem. Soc., Vol. 142, No. 4, pp. 1226-1233, Apr. 1995.